Article

Designing Nanosensors Based on Charged Derivatives of Gramicidin A

Ricardo Capone, Steven Blake, Marcela Rincon Restrepo, Jerry Yang, and Michael Mayer

J. Am. Chem. Soc., **2007**, 129 (31), 9737-9745• DOI: 10.1021/ja0711819 • Publication Date (Web): 11 July 2007

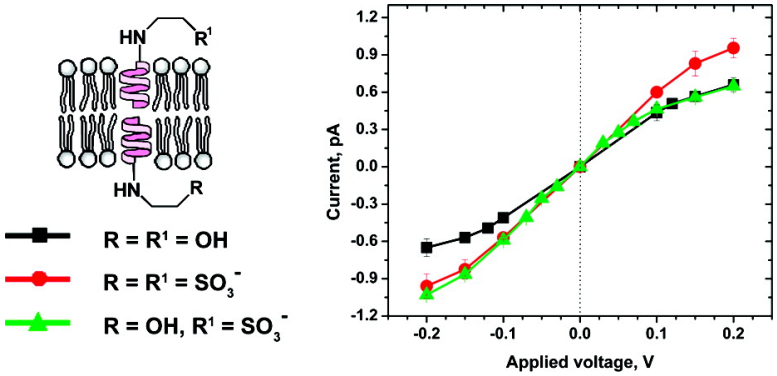

More About This Article

Additional resources and features associated with this article are available within the HTML version:

- Supporting Information
- Links to the 5 articles that cite this article, as of the time of this article download
- Access to high resolution figures
- Links to articles and content related to this article
- Copyright permission to reproduce figures and/or text from this article

View the Full Text HTML

J|A|C|S
ARTICLES
Published on Web 07/11/2007

Designing Nanosensors Based on Charged Derivatives of Gramicidin A

Ricardo Capone,[†] Steven Blake,[‡] Marcela Rincon Restrepo,[†] Jerry Yang,*[,‡] and Michael Mayer*[,†]

Contribution from Department of Chemical Engineering and Department of Biomedical Engineering, University of Michigan, 1101 Beal Avenue, Ann Arbor, Michigan 48109-2099, and Department of Chemistry and Biochemistry, University of California, San Diego, 9500 Gilman Drive, MC 0358, La Jolla, California 92093-0358

Received February 22, 2007; E-mail: mimayer@umich.edu; jerryyang@ucsd.edu

Abstract: Detection of chemical processes on a single molecule scale is the ultimate goal of sensitive analytical assays. We recently reported the possibility to detect chemical modifications on individual molecules by monitoring a change in the single ion channel conductance of derivatives of gramicidin A (gA) upon reaction with analytes in solution. These peptide-based nanosensors detect reaction-induced changes in the charge of gA derivatives that were engineered to carry specific functional groups near their C-terminus.[1] Here, we discuss five key design parameters to optimize the performance of such chemomodulated ion channel sensors. In order to realize an effective sensor that measures changes in charge of groups attached to the C-terminus of a gA pore, the following conditions should be fulfilled: (1) the change in charge should occur as close to the entrance of the pore as possible; (2) the charge before and after reaction should be well-defined within the operational pH range; (3) the ionic strength of the recording buffer should be as low as possible while maintaining a detectable flow of ions through the pore; (4) the applied transmembrane voltage should be as high as possible while maintaining a stable membrane; (5) the lipids in the supporting membrane should either be zwitterionic or charged differently than the derivative of gA. We show that under the condition of high applied transmembrane potential ($>$100 mV) and low ionic strength of the recording buffer ($\leq$0.10 M), a change in charge at the *entrance* of the pore is the dominant requirement to distinguish between two differently charged derivatives of gA; the conductance of the heterodimeric gA pore reported here does not depend on a difference in charge at the exit of the pore. We provide a simple explanation for this asymmetric characteristic based on charge-induced local changes in the concentration of cations near the lipid bilayer membrane. Charge-based ion channel sensors offer tremendous potential for ultrasensitive functional detection since a single chemical modification of each individual sensing element can lead to readily detectable changes in channel conductance.

Introduction

Derivatives of gramicidin A (gA) show promise as ultrasensitive transducers for detecting chemical and biochemical analytes because of the high amplification that is inherent to the ion channel activity of these helical peptides:[2−6] the opening of a single ion channel results in the measurable flux of 10^3 to 10^6 ions per millisecond across lipid membranes.[7] Gramicidin A is a natural ion channel-forming peptide (MW 1.9 kDa, secreted by the bacterium *Bacillus brevis*) that facilitates a transmembrane flux of monovalent cations upon reversible head-to-head dimerization in lipid bilayers.[8,9] Gramicidin A is well suited for biosensor applications because of its defined and quantized characteristics of ion channel conductance. Moreover, gA has advantages over many other ion channels or pores for development of biosensors since it can be dissolved in aqueous solutions and since it incorporates spontaneously into bilayers (as opposed to most ion channel proteins that have to be reconstituted into bilayers by proteoliposome fusion[10−13]). Once in the membrane, gA self-assembles into a functional dimeric

[†] University of Michigan.
[‡] University of California, San Diego.

(1) Blake, S.; Mayer, T.; Mayer, M.; Yang, J. *Chembiochem.* **2006**, *7*, 433−435.
(2) Andersen, O. S.; Koeppe, R. E.; Roux, B. *IEEE Trans. Nanobiosci.* **2005**, *4*, 10−20.
(3) Cornell, B. A.; Braach-Maksvytis, V. L.; King, L. G.; Osman, P. D.; Raguse, B.; Wieczorek, L.; Pace, R. J. *Nature* **1997**, *387*, 580−583.
(4) Cornell, B. A.; Braach-Maksvytis, V. L.; King, L. G.; Osman, P. D.; Raguse, B.; Wieczorek, L.; Pace, R. J. *Novartis. Found. Symp.* **1999**, *225*, 231−254.
(5) Finkelstein, A.; Andersen, O. S. *J. Membr. Biol.* **1981**, *59*, 155−171.
(6) Wallace, B. A. *J. Struct. Biol.* **1998**, *121*, 123−141.
(7) Aidley, D. J.; Stanfield, P. R. *Ion Channels: Molecules in Action*, 1st ed.; Cambridge University Press: Cambridge, UK, 1996; pp 28−31.
(8) Hladky, S. B.; Haydon, D. A. *Nature* **1970**, *225*, 451−453.
(9) Stankovic, C. J.; Heinemann, S. H.; Delfino, J. M.; Sigworth, F. J.; Schreiber, S. L. *Science* **1989**, *244*, 813−817.
(10) Diociaiuti, M.; Molinari, A.; Ruspantini, I.; Gaudiano, M. C.; Ippoliti, R.; Lendaro, E.; Bordi, F.; Chistolini, P.; Arancia, G. *Biochim. Biophys. Acta* **2002**, *1559*, 21−31.
(11) Pizzolato, F.; Morelis, R. M.; Coulet, P. R. *Quim. Anal.* **2000**, *19*, 32−37.
(12) Ohlsson, P. A.; Tjarnhage, T.; Herbai, E.; Lofas, S.; Puu, G. *Bioelectrochem. Bioenerg.* **1995**, *38*, 137−148.
(13) Miller, C. *Ion Channel Reconstitution*, 1st ed.; Plenum Press: New York, 1986; pp 131−153.

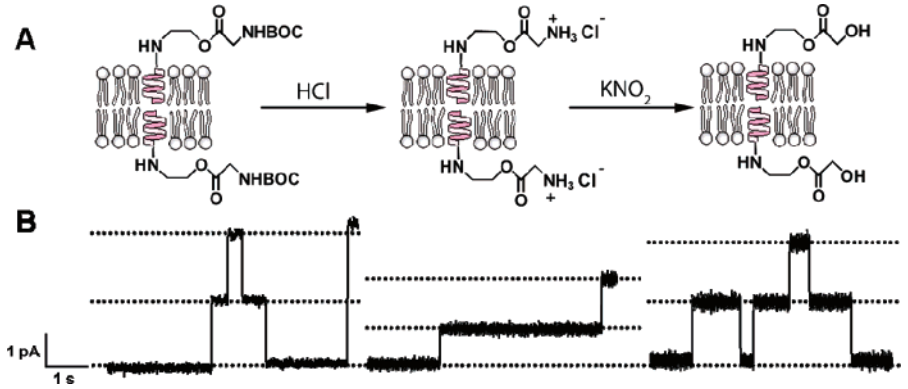

Figure 1. Monitoring transformations of chemical groups on molecules attached to the C-terminus of gramicidin A (gA) by measurement of single ion channel currents.[1] (A) Cartoon of a two-step conversion of gA carrying a *tert*-butyloxycarbonyl-protected (BOC-protected) glycine group (left) to gA carrying a glycolic acid group in the presence of externally added reagents in solution. (B) Representative single ion channel traces of the corresponding derivatives of gA shown in part A (for comparison, all three derivatives were recorded in 1.00 M KCl containing 0.01 M HEPES buffer, pH 7.4). All three current traces were obtained at the same applied potential and are shown with the same scaling of the *y*- and *x*-axis.

nanostructure with characteristic, transient ion flux.[14−16] Additional potential advantages of gA for sensor applications are (1) the commercial availability of gA in gram-scale quantities, (2) the ability to derivatize the C-terminus of gA chemically without loss of ion channel activity,[1,17,18] (3) the ability to detect changes in the single-channel conductance, γ, of gA in response to derivatization at the C-terminus,[1,18−20] and (4) the low background interference of the ion channel signal from non-ionic molecules in solution (for instance, since this ion channel-based sensor is not relying on optical detection, colored molecules in solution do not interfere as long as they do not influence the passage of monovalent cations through gA pores or alter significantly the ionic strength of the recording buffer).[21]

In order to exploit the potentially useful advantages of gA for detection purposes, several groups (including ours) have explored the use of gA for a number of sensor applications. Derivatives of gA, for instance, have been used to sense protein−ligand interactions,[3,22−25] redox potential of the electrolyte solution,[26] ammonium ions,[27] light,[28,29] and pH at membrane interfaces.[30,31] In pioneering work, Läuger's group demonstrated that charged derivatives of gA can have markedly different conductance values based on the polarity and number of the attached charges.[18,32,33] Recently, we showed that the functional properties of a chemical analyte (i.e., its reactivity with certain functional groups) can be used to change the chemical properties (i.e., the charge) of these reactive groups which were covalently attached to the opening of gA and that this change in chemical properties can be monitored *in situ* by using single ion channel recordings (Figure 1).[1,34] This proof-of-principle demonstration suggests that derivatives of gA may be useful as a platform for sensing chemical or biochemical analytes that change the charge of functional groups attached to the entrance of these semisynthetic nanopores.

In order to evaluate the usefulness and the potential of sensors that are based on detecting changes of charge at the entrance of a gA pore, we explored six parameters that influence the conductance of monovalent cations through these charge-responsive nanopores. Specifically, this paper discusses the influence of (1) the distance of the charge from the opening of the pore, (2) the ionic strength of the recording buffer, (3) the importance of a well-defined charge on the derivative of gA in the pH range of analysis, (4) the applied transmembrane voltage, (5) the molecular asymmetry of the gA dimer (e.g., homodimer versus heterodimer), and 6) the charge on the headgroups of the lipid membrane as parameters that can be optimized to maximize the performance of charge-based, chemomodulated ion channel sensors derived from gA. We provide a simple model for the behavior of conductance through the homodimeric and the heterodimeric pores of gA described in this work in

(14) Woolley, G. A.; Wallace, B. A. *J. Membr. Biol.* **1992**, *129*, 109−136.
(15) Wallace, B. A. *Annu. Rev. Biophys. Biophys. Chem.* **1990**, *19*, 127−157.
(16) Hladky, S. B.; Haydon, D. A. *Curr. Top. Membr. Transp.* **1984**, *21*, 327−372.
(17) Apell, H. J.; Bamberg, E.; Alpes, H. *J. Membr. Biol.* **1979**, *50*, 271−285.
(18) Apell, H. J.; Bamberg, E.; Alpes, H.; Lauger, P. *J. Membr. Biol.* **1977**, *31*, 171−188.
(19) Pfeifer, J. R.; Reiss, P.; Koert, U. *Angew. Chem., Int. Ed.* **2006**, *45*, 501−504.
(20) Borisenko, V.; Lougheed, T.; Hesse, J.; Fureder-Kitzmuller, E.; Fertig, N.; Behrends, J. C.; Woolley, G. A.; Schutz, G. J. *Biophys. J.* **2003**, *84*, 612−622.
(21) With regards to interference, several characteristics of gA pores are important to consider: Only small monovalent cations (e.g., monovalent metal ions or protons) can pass through gA channels. Divalent cations such as Ca^{2+} are known to block gA channels at concentrations ≥100 mM (see Bamberg, E.; Lauger, P. *J. Membr. Biol.* **1977**, *35*, 351−375). Large concentrations of monovalent cations or divalent cations from analytical samples can therefore be expected to cause interference. Molecules larger than 5 Å cannot pass since gA channels have a diameter of ∼4 Å; these large molecules are not expected to cause significant interference (regardless of whether they are colored or fluorescent) as long as they cannot block gA pores. Therefore, the presence of significant concentrations of monovalent or divalent cations should be accounted for when measuring the conductance of gA derivatives (for instance by calibration or standard addition). It is also important to note that *reactions* that lead to a significant change of the ionic strength of the solution may also require correction or calibration.
(22) Futaki, S.; Zhang, Y.; Kiwada, T.; Nakase, I.; Yagami, T.; Oiki, S.; Sugiura, Y. *Bioorg. Med. Chem.* **2004**, *12*, 1343−1350.
(23) Hirano, A.; Wakabayashi, M.; Matsuno, Y.; Sugawara, M. *Biosens. Bioelectron.* **2003**, *18*, 973−983.
(24) Sugawara, M.; Hirano, A.; Buhlmann, P.; Umezawa, Y. *Bull. Chem. Soc. Jpn.* **2002**, *75*, 187−201.
(25) Antonenko, Y. N.; Rokitskaya, T. I.; Kotova, E. A.; Reznik, G. O.; Sano, T.; Cantor, C. R. *Biochemistry.* **2004**, *43*, 4575−4582.
(26) Antonenko, Y. N.; Stoilova, T. B.; Kovalchuk, S. I.; Egorova, N. S.; Pashkovskaya, A. A.; Sobko, A. A.; Kotova, E. A.; Surovoy, A. Y. *Biochim. Biophys. Acta.* **2006**, *1758*, 493−498.
(27) Nikolelis, D. P.; Siontorou, C. G. *Anal. Chem.* **1996**, *68*, 1735−1741.
(28) Stankovic, C. J.; Heinemann, S. H.; Schreiber, S. L. *Biochim. Biophys. Acta* **1991**, *1061*, 163−170.
(29) Banghart, M. R.; Volgraf, M.; Trauner, D. *Biochemistry* **2006**, *45*, 15129−15141.
(30) Borisenko, V.; Zhang, Z.; Woolley, G. A. *Biochim. Biophys. Acta* **2002**, *1558*, 26−33.
(31) Bamberg, E.; Alpes, H.; Apell, H. J.; Bradley, R.; Harter, B.; Quelle, M. J.; Urry, D. W. *J. Membr. Biol.* **1979**, *50*, 257−270.
(32) Bamberg, E.; Apell, H. J.; Alpes, H.; Gross, E.; Morell, J. L.; Harbaugh, J. F.; Janko, K.; Lauger, P. *Fed. Proc.* **1978**, *37*, 2633−2638.
(33) Apell, H. J.; Bamberg, E.; Lauger, P. *Biochim. Biophys. Acta* **1979**, *552*, 369−378.

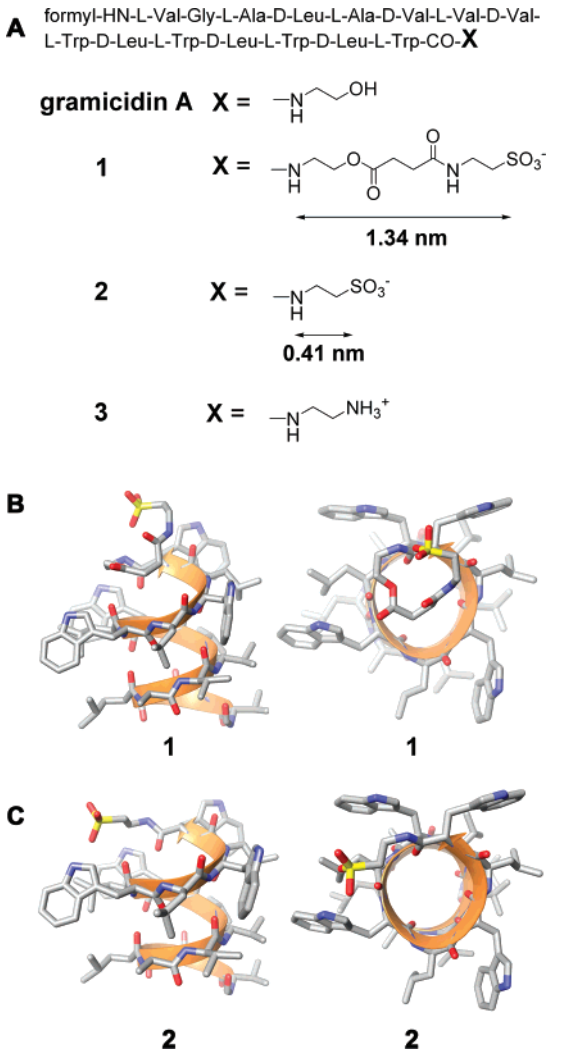

Figure 2. Sequence and calculated structure of two negatively charged derivatives of gramicidin A (gA). (A) Sequence of gA, of a negatively charged sulfonate group covalently attached to gA via a long spacer (**1**), a negatively charged sulfonate group covalently attached to gA via a short spacer (**2**), and a positively charged amine group covalently attached to gA via a short spacer (gramicidamine, **3**). The lengths shown for the spacers in **1** and **2** (from the nitrogen atom to the sulfur atom) were estimated by energy minimization in their fully extended conformation. (B) Computer-generated side view (left) and top view model (right) of **1** based on molecular mechanics calculations. (C) Computer-generated side view (left) and top view model (right) of **2** based on molecular mechanics calculations.

the presence of an applied potential. This model is in excellent agreement with the experimental results. Furthermore, we explore mass transport of ions as a plausible limiting factor for conductance through gA pores under conditions of low KCl concentration and large applied potential.

Results and Discussion

Influence of the Distance of Charged Residues from the Opening of the Pore on the Conductance of Derivatives of gA. In order to investigate the influence of the distance of a charged group attached to the entrance of a gA pore on the single channel conductance, we synthesized two sulfonate derivatives of gA (Figure 2A): one with a long spacer, **1**, and one with a short spacer, **2**.[35] We chose a sulfonate group for these studies because it maintains a constant negative charge over a wide pH range (since the pK_a of a sulfonate group is <0). Figure 2B and 2C show the energy minimized structures of **1** and **2**, respectively, as computed from a conformational search based on molecular mechanics calculations using Macromodel software. From the conformations shown in Figure 2B and 2C, we compared the location of the negative charge in **1** and **2** by measuring the distance of the sulfur atoms to a fixed point in space near the opening of the pore (located at half the distance between the α-carbon of Leu14 and the α-carbon of Trp11). From this comparison, the molecular mechanics calculations estimate that the sulfonate group of **1** is 0.75 nm and the sulfonate group of **2** is 0.68 nm from this fixed point at the opening of the pore. If we measure the distance of the sulfur atoms in **1** and **2** with the spacers in fully extended conformation, we estimate the charge of the sulfonate group in **1** to be located at a maximum distance of 1.81 nm and in **2** to be located at a maximum distance of 0.88 nm from this same fixed point near the opening of the pore. Although these charged derivatives of gA are likely to adopt dynamically a number of conformations with fluctuating distances of the charge from the pore when incorporated in a bilayer setup, these calculations are qualitatively consistent with the reasonable prediction that, on average, the charge in **1** is located further away (0.75−1.81 nm) from the opening of the pore compared to the charge in **2** (0.68−0.88 nm).

Figure 3 shows representative traces of the currents generated from different derivatives of gA at an applied potential of 150 mV in a recording buffer containing 0.02 M KCl: the difference in conductance of ions through pores formed from gA-gA, **1-1**, or **2-2** resulted from the difference in magnitude (i.e., no charge versus negative charge)[18,31] and distance of the charge attached near the entrance of the pore. These distinct conductance values are consistent with our recent report of using derivatives of gA to detect chemical reactions that resulted in a difference in charge of functional groups attached to the opening of these pores.

Figure 3 demonstrates that the conductances of pores of **1-1,** and **2-2** are measurably different from the conductance of pores of gA-gA and illustrates that this difference is bigger when the negative charge is located close to the entrance of the pore (**2**) compared to a charge that is located further away (**1**). According to the Debye−Hückel theory,[36] the electrostatic attraction between oppositely charged species near a charged surface is distance dependent. In addition, this theory predicts that the electrostatic attraction of cations in solution by the negative sulfonate group in **1** and **2** decreases with increasing ionic strength of the electrolyte solution (because of the small double-layer thickness and the corresponding enhanced shielding of the negative charge in solutions with increased concentrations of ions).[36] We tested this hypothesis by comparing the ion channel conductance of gA, **1**, and **2** in recording buffers with different ionic strengths.

(34) Bayley and coworkers have shown previously that a different pore, the α-hemolysin pore, can also be used to detect chemical reactions by changes in single-channel conductance. The changes in conductance were, however, typically due to steric changes (i.e., partial blockage) in the α-hemolysin pore and not due to changes in charge. See Bayley, H.; Cremer, P. S. *Nature* **2001**, *413*, 226−230; Luchian, T.; Shin, S. H.; Bayley, H. *Angew. Chem., Int. Ed.* **2003**, *42*, 3766−3771; Luchian, T.; Shin, S. H.; Bayley, H. *Angew. Chem., Int. Ed.* **2003**, *42*, 1925−1929; Shin, S. H.; Luchian, T.; Cheley, S.; Braha, O.; Bayley, H. *Angew. Chem., Int. Ed.* **2002**, *41*, 3707−3709.

(35) Roeske, R. W.; Hrinyopavlina, T. P.; Pottorf, R. S.; Bridal, T.; Jin, X. Z.; Busath, D. *Biochim. Biophys. Acta* **1989**, *982*, 223−227.

(36) Hamann, C. H.; Hamnett, A.; Wolf, V. *Electrochemistry*, 1st ed.; Wiley-VCH: Weinheim, Germany, 1998; pp 36−44.

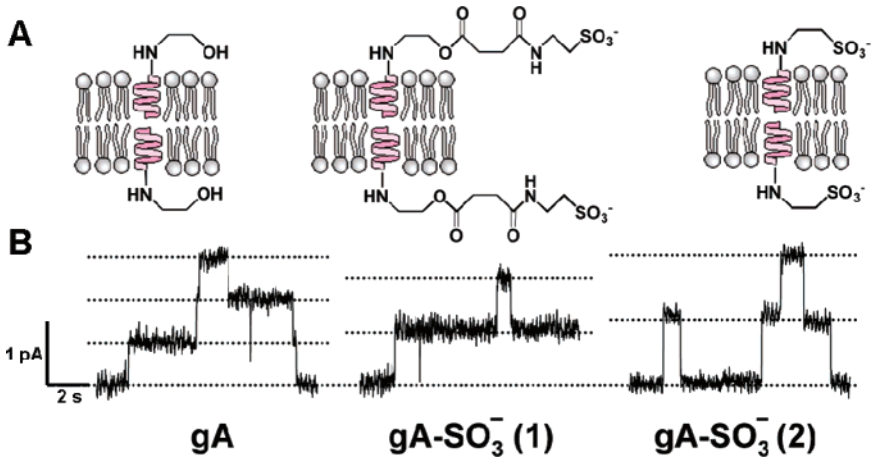

Figure 3. Cartoon of gA pores in planar lipid bilayers and current versus time traces of the respective dimeric pores. (A) Cartoon representation of homodimeric pores of gA-gA, **1-1**, and **2-2** in a bilayer and (B) corresponding representative ion channel traces of pores of gA-gA, **1-1**, and **2-2**. All three traces were obtained at an applied potential of +150 mV from lipid bilayers made with 1,2-diphytanoyl-*sn*-glycero-3-phosphocholine (DiPhyPC) in an electrolyte containing 0.02 M KCl buffered with 0.2 mM HEPES at pH 7.4. Note the increased single channel conductance of pores of **1-1** compared to gA-gA and of **2-2** compared to **1-1** and gA-gA. All current traces are shown with the same scaling of *y*- and *x*-axis after low-pass filtering with a digital Gaussian filter with a cutoff frequency of 30 Hz.

Table 1. Single-Channel Conductances, γ, of Homodimers of gA-SO_3^- with a Long Spacer Arm (**1**) and of gA-SO_3^- with a Short Spacer Arm (**2**) Compared to Native gA at Different Concentrations of KCl in the Recording Electrolyte (buffered with HEPES to pH 7.4)[a]

concn of KCl (M)	γ, gA-gA (pS)	γ, **1-1** (pS)	γ, **2-2** (pS)	γ-ratio, **1-1**/gA-gA	γ-ratio, **2-2**/gA-gA
0.01	2.7 ± 0.5	3.5 ± 0.3	4.3 ± 0.3	1.3	1.6
0.10	10.3 ± 0.1	11.0 ± 0.4	12.6 ± 0.4	1.1	1.2
1.00	20.0 ± 0.2	19.5 ± 0.4	21.5 ± 0.3	1.0	1.1

[a] Bilayers were made from DiPhyPC lipids. Conductances were obtained from the slope of current versus voltage curves (I−V curves) in the linear range $\leq|\pm 100$ mV$|$ of the I−V curves. Errors represent the standard deviation calculated from at least two (typically three) independent experiments. 1 pS $= 1 \times 10^{-12}\ \Omega^{-1}$. A two sample *t*-test and a one-way ANOVA test both confirmed that (in recording buffer containing 0.01 M KCl and in recording buffer containing 0.10 M KCl) the mean conductance values of gA-gA, **1-1**, and **2-2** were all significantly different from each other with a significance level of 0.05.

Influence of the Ionic Strength of the Recording Buffer on the Conductance of Negatively Charged Derivatives of gA. Table 1 shows the single-channel conductance of homodimers of gA and of negatively charged gA derivatives **1** and **2**. The effect of the negative charge on the gA derivatives with respect to their single-channel conductance decreased with increasing ionic strength of the solution, as predicted by the Debye−Hückel theory.[36] We found the biggest relative difference in conductance between homodimers of **2** and homodimers of gA when we used a buffer with a concentration of 0.01 M KCl. At this concentration, the conductance of **2-2** was a factor of 1.6 larger than that of gA-gA. Even at a concentration of 0.10 M KCl, the single-channel conductance of **2-2** was a factor of 1.2 greater than the conductance of gA-gA. On the other hand, at a concentration of 1.00 M KCl, the difference in single channel conductance between gA-gA and **2-2** was below 10% (Table 1). In the case of derivative **1** (with the negative sulfonate group attached to gA by a longer spacer length compared to **2**) the effect of screening electrostatic attraction was more pronounced compared to gA derivative **2**: at low ionic strength (0.01 M KCl) the difference in conductance compared to gA was greater by a factor of 1.3; at 0.10 M KCl and 1.00 M KCl the difference was 7% and 3%, respectively. For the two sulfonate derivatives of gA explored here, the difference in charge compared to gA appeared to dominate the single channel conductance over any other differences in chemical properties such as the size (i.e., bulkiness) of the attached group.[1] On the basis of the results from Table 1, KCl concentrations lower than 0.01 M could be expected to further enhance the difference in conductance between the negatively charged gA derivatives and the original, uncharged gA. We found, however, that the formation of stable lipid bilayers from zwitterionic lipids was difficult at these low KCl concentrations.[37] In order to obtain reliable and reproducible recording conditions, we found that KCl concentrations of at least 0.01 M (preferably $\geq$0.02 M) worked best for the ion channel experiments described here.

Importance of a Well-Defined Charge on the Derivative of gA in the pH Range of Analysis. Since the charge on functional groups attached to gA may depend on the protonation state of the molecule, it is important to consider the pK_a of functional groups in the design of a charge-based gA sensor. To demonstrate the importance of a well-defined charge on the gA derivative at the pH range of analysis, we compared the conductance of pores from **2-2** with the conductance of pores from gA-gA at pH 7.4 and pH 12 (Table 2). As expected, we found that the conductance of pores from **2-2** was significantly larger than the conductance from gA-gA at both pH values (because of the presence of the sulfonate group on **2**, which was charged negatively at both pH values since its pK_a in water is $<$0). To provide an example of a functional group whose charge is not well-defined over the same pH range, we synthesized an amine-terminated derivative of gA (gramicidamine, **3**, see Figure 2). This basic derivative of gA is

(37) We conducted the experiments shown in Table 1 by using "folded" and "painted" bilayers (for details, see Materials and Methods). We tested whether the two methods result in differences in the single-channel conductances of the same pores. We did not observe significant differences in conductance; however, the average relative standard deviation of the conductances was smaller in folded bilayers than in painted bilayers (2.4% versus 5.5%). This difference is expected since folded bilayers are "solvent-free", more precisely; decane is typically replaced by hexadecane, which partitions less into the bilayer than decane, and thus folded bilayers result in thinner membranes that are typically considered better models of biological bilayers than painted bilayers. Therefore, in order to maximize the sensitivity of sensors that measure changes in the single channel conductance of gA, folded bilayers are preferable. It is, however, possible to use painted bilayers if sensor simplicity is important.

Table 2. Single-Channel Conductances, γ, of Homodimers of gA, **2**, and **3** at pH 7.4 and pH 12[a]

composition of pore	γ at pH 7.4 (pS)	γ at pH 12 (pS)
gA-gA	4.5 ± 0.1	7.8 ± 0.2
2-2	5.8 ± 0.1	9.8 ± 0.2
3-3	3.8 ± 0.2	7.7 ± 0.9

[a] Bilayers were made from DiPhyPC lipids in 20 mM KCl. For the measurements at pH 12, 10 mM KOH was added to this electrolyte to give the desired pH. Conductances were obtained from the slope of current versus voltage curves (I−V curves) in the linear range $\leq|\pm 100$ mV| of the I−V curves.

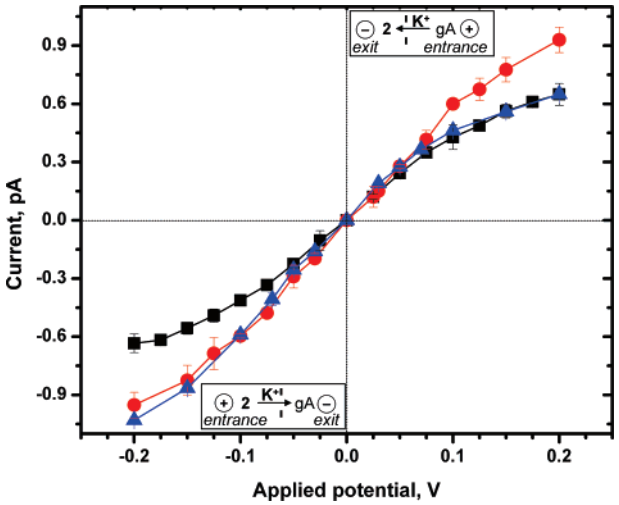

Figure 4. Current−voltage characteristic of a homodimeric pore of gA-gA (■), **2-2** (red ●), and a heterodimeric, asymmetric pore of gA and **2** (blue ▲). The heterodimeric, asymmetric pore was assembled by adding native gA to the cis compartment and **2** to the trans compartment of the bilayer setup[44] (the cis compartment refers to the compartment that defined the polarity of the applied voltage, the trans compartment was connected to ground). The concentration of KCl was 0.02 M for these experiments, and bilayers were formed with DiPhyPC lipids using the folding method. Each data point represents the average of at least three measurements of current.[66] The annotations of gA and **2** in the boxes of the graph indicate the direction of the flux of K^+ ions (arrows) and thus illustrate whether gA or **2** was at the entrance or at the exit of the pore at a given polarity of the applied voltage.

expected to be predominantly protonated (and hence positively charged) at pH 7.4 and predominantly uncharged at pH 12 (since the pK_a of a primary amine in water is ∼10). When we compared the conductance of pores from **3-3** with the conductance of pores from gA-gA at pH 7.4 (Table 2), we found, as expected, that the conductance of **3-3** was significantly smaller than the conductance of gA-gA (presumably because of the positively charged amine group on **3**). In contrast, at pH 12, the predominant conductance of **3-3** was indistinguishable from the conductance of gA-gA (presumably because of the neutral character of the unprotonated amine group). These results demonstrate that it is important to design charge-based sensors such that there is a measurably different conductance between the two derivatives of gA at the operational pH.

Dependence of the Current−Voltage Characteristic of gA Channels on the Applied Transmembrane Voltage and on the Molecular Heterogeneity of the gA Dimers. Figure 4 demonstrates that the absolute difference in conductance between gA and its negatively charged derivative **2** increased with increasing transmembrane potential in a recording buffer containing 0.02 M KCl. Figure 4 also shows that the current through all gA pores did not increase linearly with applied voltages above 100 mV. We observed this nonlinear behavior only at low KCl concentrations (≤0.10 M KCl). At a concentration of 1.00 M KCl, the I−V curve of gA, as expected, was linear (data not shown). One possible explanation for the nonlinear behavior of the I−V curve of gA and its negatively charged derivatives at low KCl concentrations is that the flux of ions through the pore was sufficiently fast that the supply of potassium ions to the pore started to become rate limiting at high applied potentials (>100 mV) for the overall rate of ion transport.[38] We, therefore, expected that a negatively charged group that is able to increase the local concentration of potassium ions close to the entrance of the pore because of electrostatic attraction should result in an increase in conductance compared to native gA under the same applied potential. This increase should be most pronounced at low ionic strength of the bulk solution (here at low concentration of KCl) and under conditions where the supply of ions to the pore is starting to become a limiting factor (for example at high transmembrane voltages when the movement of the ions through the pore is sufficiently fast). The results in Figure 4 are consistent with these predictions. The relative difference in conductance between the negatively charged gA derivatives compared to gA increased with increasing transmembrane voltage; the ratio between the conductance of **2-2** and gA-gA (at a KCl concentration of 0.02 M), for instance, increased from 1.4 at 100 mV to 1.5 at 200 mV applied potentials.

Because of our interest in developing sensors based on changing the charge of chemical groups attached to the entrance of a gA pore, we explored whether it was necessary for the gA derivatives used here to change the charge of both gA monomers in a dimeric pore in order to observe a measurable change in conductance. We, therefore, investigated the conductance behavior of a heterodimeric gA pore (Figure 4). These asymmetric heterodimeric pores were composed of gA in one leaflet of the bilayer (here, the leaflet facing the aqueous compartment that defined the polarity of the applied voltage, denoted as the cis compartment) and of **2** in the opposite leaflet of the bilayer (denoted as the trans compartment). The question was, would the I−V curve of these heterodimeric pores be the same as the I−V curve of homodimeric pores of gA, or would it be similar to the I−V curve of homodimeric pores of **2** or would it be different than the I−V curves of either homodimeric pore? We found (Figure 4) that at transmembrane potentials above 100 mV, the I−V characteristic of heterodimeric pores was dominated by the charge on the gA derivative that was located at

(38) To rationalize our interpretation of nonlinear I−V curves at low ionic strength, we approximated the mass transport limited maximum current through a gA pore (diameter ∼ 4 Å) as the diffusion limited current that can be measured by a disk-shaped nanoelectrode (with a radius $r = 2 \times 10^{-10}$ m) due to the reduction or oxidation of an electroactive species (with one transferred electron per reaction, $n = 1$). In analogy to the electroactive species reacting instantaneously at the nanoelectrode surface, we assumed that K^+ ions that reach the opening of gA pore are instantaneously driven through the pore by the applied electric field. Using a concentration of $c = 20$ mol m^{-3} (20 mM) K^+ ions that have a diffusion constant of $D = 1.96 \times 10^{-9}$ m^2 s^{-1} and an equation that describes the steady state limiting current (i) of a nanodisk electrode: $i = 4nFDcr$ where $F = 96{,}485$ C is the Faraday constant (from Bard, A. J.; Faulkner, L. R. *Electrochemical Methods, Fundamentals and Applications*, 2nd ed.; John Wiley & Sons: New York, 2001; p 171), we predict that the maximum achievable, mass transport limited current through a gA pore in a solution with 20 mM K^+ ions is ∼3 pA. Since this maximum current will be approached asymptotically with increasing potentials, it is reasonable that the measured currents will deviate from ohmic behavior (current = applied potential × conductance) at potentials that are not sufficiently large to reach this mass transport limited current of 3 pA (for instance, at 200 mV applied potential in Figure 4, the current through **2-2** was ∼30% of this estimated maximum, mass transport limited current).

the entrance of the pore; it was not affected by the charge on the gA derivative at the exit of the pore. In other words, if the polarity of the applied potential was such that the negatively charged gA derivative **2** was located at the entrance of the pore for K^+ ions (i.e., **2** added to the positively polarized compartment) while native gA was located at the exit of the pore (i.e., gA added to the negatively polarized compartment), then the overall conductance was approximately the same as that of homodimeric pores from **2**. Switching the polarity and thus placing **2** at the exit of the pore and gA at the entrance of the pore resulted in a single-channel conductance that was similar to homodimeric pores of gA.

To provide one possible explanation for the observed conductance behavior of heterodimeric pores, we considered once again the local ion concentrations near the membrane due to the presence of the negative charge on molecule **2**. Molecule **2**, in a heterodimeric pore, will, according to Debye−Hückel theory, increase the local concentration of K^+ ions close to the side of the pore that is made up by **2**. The gA molecule in the heterodimeric pore in the opposite leaflet of the bilayer will not, however, influence significantly the local concentration of K^+ ions near the membrane (since gA is not charged). Hence, if the polarity of the electric field is such that **2** is located at the entrance of the heterodimeric pore, the local increase in K^+ ions will result in an increased conductance and the ensuing conductance can be expected to be similar to homodimeric pores of **2-2**.[39] On the other hand, if the polarity of the electric field is such that gA is located at the entrance of the heterodimeric pore, the concentration of K^+ ions at the entrance is not increased and the conductance of such a pore can be expected to be similar to homodimeric pores of gA-gA. The data in Figure 4 are in excellent agreement with the predictions from this simple model.

Influence of Charge on the Lipid Headgroups on the Single Channel Conductance of gA and Its Derivatives. In order to investigate the single channel conductance of the different gA derivatives in neutral, negatively charged, and positively charged planar bilayers in the lowest possible KCl concentration, we formed bilayers in 0.01 M or 0.02 M KCl. As shown in Figure 5, the negative charges on the headgroups of lipids in bilayers neutralized the difference observed in Figure 4 in single channel conductance between gA-gA, **1-1**, and **2-2** almost completely.[40]

Figure 5 demonstrates that negative charges on the lipid membrane can override the effect of the negative charge on the sulfonate group of derivatives **1** or **2** even at concentrations of low ionic strength (here, 0.01 M). On the other hand, in bilayers that were made with neutral (zwitterionic) DiPhyPC lipids, the single channel conductance of **2-2** was significantly different

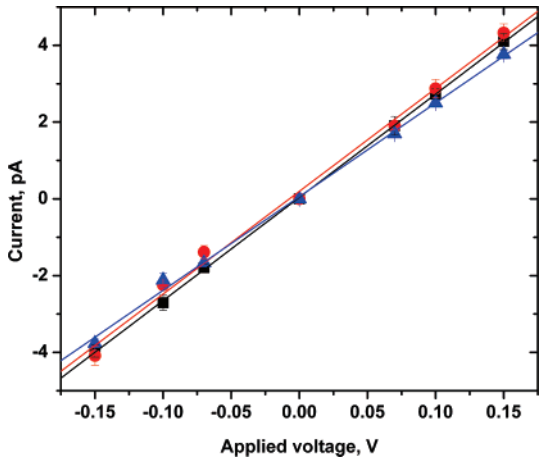

Figure 5. Effect of charge on the head group of the lipids in planar bilayers. Current−voltage characteristics of homodimeric pores of gA (■), **1** (red ●), and **2** (blue ▲) in negatively charged bilayers at low ionic strength. Planar bilayers were made with 50% zwitterionic 1-palmitoyl-2-oleoyl-*sn*-glycero-3-phosphoethanolamine (POPE) and 50% negatively charged 1,2-dioleoyl-*sn*-glycero-3-phospho-L-serine (DOPS). All experiments were performed in 0.01 M KCl with 0.1 mM HEPES (pH = 7.4) as electrolyte. Each data point represents the average of at least three mean current values calculated from fitting a Gaussian distribution to histograms of the current from original current versus time traces.

from the conductance of gA-gA pores at low ionic strength (Table 1). Only at high ionic strength (1.00 M KCl) were the conductances of pores of **2-2** in zwitterionic lipid membranes approximately the same the as pores of gA-gA.

An interesting aspect of the conductance in negatively charged membranes (50% DOPS, 50% POPE) is that the conductance values of homodimers of gA and its derivatives are increased compared to zwitterionic membranes. This observation is consistent with the prediction that permanent negative charges near the entrance of the pore increase the local concentration of cations. This increase in concentration results in increased flux of K^+ ions through the pores, and this effect can be caused by charges at the entrance of the pore such as in **2** or by charges on the surrounding membrane lipids close to the entrance of the pore.

Figure 5 shows that, at a concentration of 0.01 M KCl, the effect of electrostatic attraction of ions to the bilayer predicted by the Debye−Hückel theory is very strong to the point that the conductance of gA-gA pores (27 pS) in 50% DOPS bilayers is higher than the conductance of gA-gA (20 pS) in zwitterionic bilayers made with DiPhyPC in an electrolyte containing 1.00 M KCl. Similar results have been reported previously for gA in charged lipids,[33,41] and these observations emphasize the necessity of using appropriately charged lipid headgroups in the bilayers for development of sensitive charge-based sensors from gA.

Interestingly, when we measured the conductance of gA-gA and **2-2** in lipid bilayers that contained 10% of a lipid with positively charged headgroups (here, 1,2-dioleoyl-3-(dimethylamino)propane, DODAP, and 90% DiPhyPC), we found that the relative ratio of conductance of **2-2** to gA-gA was 10% larger than the relative ratio of conductance of these two homodimeric ion channels in purely zwitterionic lipids (both were measured in 20 mM KCl). These results show that using membranes that are oppositely charged than the gA derivatives makes it possible

(39) This model assumes that the concentration gradient of K^+ ions across asymmetric **2**-gA pores did not significantly alter the electrochemical driving force of K^+ ions through the pore. Since the part of the I−V curve of **2**-gA, in which **2** is located at the entrance of the pore, is similar to the I−V curve of **2-2** (Figure 4), this assumption appears to be justified.

(40) The differences in conductance measured for **2-2** (γ = 24.4 ± 0.5 pS) compared to gA-gA (γ = 26.9 ± 0.2 pS) or **1-1** (γ = 26.8 ± 0.9 pS) when measured in bilayers containing lipids with negatively charged headgroups are probably due to differences in chemical/physical properties other than charge (e.g., bulkiness). Since the relatively bulky sulfonate group in **2** is located closer to the opening of the pore compared to in **1** (see Figure 2), one might expect a slightly reduced conductance of ions through channels of **2-2** compared to **1-1** or gA-gA (as apparent in Figure 5) under experimental conditions in which the effect of the charge on the sulfonate groups on **1** and **2** is overridden by the negative charges of the lipids in the membrane.

(41) Rostovtseva, T. K.; Aguilella, V. M.; Vodyanoy, I.; Bezrukov, S. M.; Parsegian, V. A. *Biophys. J.* **1998**, *75*, 1783−1792.

to enhance the relative difference in conductance between the charged and uncharged pores compared to measurements in zwitterionic lipids.

Thus, to maximize the effect of the change in charge of gA derivatives for sensor applications, the lipid headgroups in the bilayers should be zwitterionic or oppositely charged than the gA derivatives used for sensing.

Conclusion

Implementing the key design parameters and experimental conditions outlined in this paper in order to sense changes in the single-channel conductance of gA-based ion channels makes these semisynthetic nanopores an excellent platform for development of sensors. Specifically, gA is readily available in gram-scale quantities,[42] it is conducive to synthetic derivatization, and it is simple to use because of its spontaneous self-incorporation into bilayers and its discrete conductance values. In addition, assays based on gA can be inexpensive, amenable to miniaturization, and potentially portable.[43−47] Although the conditions outlined in this paper are focused on the development of charge-based sensors, chemical or physical properties other than charge (i.e., steric hindrance) may also be useful for designing gA-based sensors.[48] The exquisite sensitivity of single ion channel recordings (typical concentrations for gA used in single channel recordings in commercial bilayer chambers with 1 mL volume are 1−100 pM) makes it possible to perform more than one million assays from 1 mg of gA-based nanoprobes. Current challenges for successful implementation of ion channel-based sensors are limited mechanical stability and requirement for manual preparation of planar lipid bilayers.[49] Recent advances in microfabrication techniques, however, make it possible to form bilayers in an automated fashion[43,45,50−58] as well as to prepare bilayers with improved mechanical stability by forming bilayers over pores with diameters below 15 μm[44,59,60] or by embedding bilayers in hydrogels.[61,62] A practical platform for using synthetically tailored gramicidin derivatives with distinct conductance properties may, therefore, be within reach for the ultrasensitive and selective detection of chemically or biochemically reactive analytes in solution.

Experimental Section

Materials. We purchased all reagents and chemicals from Sigma-Aldrich unless otherwise stated. Gramicidin A (gA) was purchased from Cal Biochem (97% purity). The following lipids were purchased from Avanti Polar Lipids, Inc.: 1,2-diphytanoyl-*sn*-glycero-3-phosphocholine (DiPhyPC); 1,2-dioleoyl-*sn*-glycero-3-[phospho-L-serine] (DOPS); 1-palmitoyl-2-oleoyl-*sn*-glycero-3-phosphoethanolamine (POPE); 1,2-dioleoyl-3-(dimethylamino)propane (DODAP).

Synthesis of Gramicidyl Succinic Acid. We dissolved 6 mg of gA (3.2 μmol) in 0.5 mL of dichloromethane (DCM). We added 2.6 μL (32 μmol) of pyridine and 3.2 mg (32 μmol) of succinic acid to the solution of gA. To increase the solubility of succinic acid, a few drops of tetrahydrofuran (THF) were added. The solution was stirred for 12 h at 23 °C. After concentration of the solution *in vacuo*, the desired product was isolated by chromatography over silica using a 9:1 mixture of DCM/methanol (MeOH) as eluent. The desired product had an R_f value of 0.3 (for comparison, gA had an R_f value of 0.5) using the same eluent. The product was taken directly to the next step without further characterization.

Synthesis of Gramicidyl Taurinyl Succinate (1). We dissolved 2.6 mg (1.3 μmol) of gramicidyl succinic acid and 0.17 μL (1.3 μmol, from a stock solution in THF) of *tert*-butyl chloroformate in 1 mL of anhydrous THF. The solution was stirred for 10 min at −20 °C. Then 0.15 μL (1.3 μmol, from a stock solution in THF) of diisopropylethylamine was added, and the flask was flushed with N_2. The reaction was stirred at 0 °C for 30 min, and 0.02 mL of an aqueous 16 mg mL^{-1} solution of taurine (2.6 μmol) was added to the mixture. The mixture was stirred at 0 °C for 3 h, warmed to 23 °C, and then stirred for an additional 10 h. The solution was concentrated *in vacuo*, and the product was isolated in 28% yield by chromatography over silica using a 9:1 mixture of DCM/MeOH as eluent. The desired product had an R_f value of 0.1 in the same eluent. ESI-MS showed a peak at $m/z = 2090.48$ corresponding to the expected $[M + H]^+$ of **1**.

Synthesis of 2-Aminoethyl Gramicidate. We prepared 2-aminoethyl gramicidate using a modified procedure that was previously reported in the literature.[63] We dissolved 12.4 mg (6.3 μmol) of gA in 0.25 mL of anhydrous acetonitrile. We added 25 μL (260 μmol) of $POCl_3$ to the solution of gA. The reaction was stirred at 23 °C for 4 h. The solution was concentrated *in vacuo*. The mixture was then dissolved in 1 mL of 10% H_2O in acetonitrile and stirred for 30 min. After concentrating the solution again *in vacuo*, the mixture was dissolved in 1.5 mL of 2:1 DCM/MeOH, and the resulting solution was added dropwise to 50 mL of H_2O. The precipitate was collected on filter paper to yield 97% of crude product based on gA. ESI-MS in negative mode revealed a major peak at $m/z = 1880.85$ corresponding to the $[M - H]^-$ of the product.

Syntheis of 2-Hydroxyethyl Gramicidate. We dissolved 5.2 mg of crude 2-aminoethyl gramicidate in 0.15 mL of acetonitrile and 0.45 mL of acetate buffer (0.5 M, pH 3.9) and stirred for 5 min at 23 °C. We added 30 mg of $NaNO_2$ to the solution, and the reaction was stirred for 7 h at 23 °C. The mixture was concentrated *in vacuo* and dissolved in 0.5 mL of 2:1 DCM/MeOH. The solution was added dropwise to 50 mL of H_2O. The resulting precipitate was collected to yield 95% of

(42) Stankovic, C. J.; Delfino, J. M.; Schreiber, S. L. *Anal. Biochem.* **1990**, *184*, 100−103.
(43) Schmidt, C.; Mayer, M.; Vogel, H. *Angew. Chem., Int. Ed.* **2000**, *39*, 3137−3140.
(44) Mayer, M.; Kriebel, J. K.; Tosteson, M. T.; Whitesides, G. M. *Biophys. J.* **2003**, *85*, 2684−2695.
(45) Mayer, M.; Terrettaz, S.; Giovangrandi, L.; Vogel, H. In *Biosensors: A practical approach*, 2nd ed.; Cooper, J. M.; Cass, A. E. G., Eds.; Oxford University Press: Oxford, 2003; pp 153−184.
(46) Laiwalla, F.; Klemic, K. G.; Sigworth, F. J.; Culurciello, E. *IEEE Trans. Circuits Syst. I, Reg. Papers* **2006**, *53*, 2364−2370.
(47) Sondermann, M.; George, M.; Fertig, N.; Behrends, J. C. *Biochim. Biophys. Acta* **2006**, *1758*, 545−551.
(48) In these circumstances, recording buffers of high ionic strength may be used and possibly result in improved performance compared to the low ionic strength buffers that are required for charge-based sensing. Using buffers with high ionic strength may be beneficial to reduce possible interference from cations in real samples.
(49) Terrettaz, S.; Mayer, M.; Vogel, H. *Langmuir* **2003**, *19*, 5567−5569.
(50) Malmstadt, N.; Nash, M. A.; Purnell, R. F.; Schmidt, J. J. *Nano Lett.* **2006**, *6*, 1961−1965.
(51) Funakoshi, K.; Suzuki, H.; Takeuchi, S. *Anal. Chem.* **2006**, *78*, 8169−8174.
(52) Chen, C. C.; Folch, A. *Lab Chip.* **2006**, *6*, 1338−1345.
(53) Craighead, H. *Nature* **2006**, *442*, 387−393.
(54) Suzuki, H.; Tabata, K. V.; Noji, H.; Takeuchi, S. *Langmuir* **2006**, *22*, 1937−1942.
(55) Klemic, K. G.; Klemic, J. F.; Sigworth, F. J. *Pfluegers. Arch.* **2005**, *449*, 564−572.
(56) Romer, W.; Lam, Y. H.; Fischer, D.; Watts, A.; Fischer, W. B.; Goring, P.; Wehrspohn, R. B.; Gosele, U.; Steinem, C. *J. Am. Chem. Soc.* **2004**, *126*, 16267−16274.
(57) Fertig, N.; Blick, R. H.; Behrends, J. C. *Biophys. J.* **2002**, *82*, 3056−3062.
(58) Pantoja, R.; Sigg, D.; Blunck, R.; Bezanilla, F.; Heath, J. R. *Biophys. J.* **2001**, *81*, 2389−2394.
(59) Peterman, M. C.; Ziebarth, J. M.; Braha, O.; Bayley, H.; Fishman, H. A.; Bloom, D. M. *Biomed. Microdevices* **2002**, *4*, 231−236.
(60) Bayley, H.; Cremer, P. S. *Nature* **2001**, *413*, 226−230.
(61) Jeon, T. J.; Malmstadt, N.; Schmidt, J. J. *J. Am. Chem. Soc.* **2006**, *128*, 42−43.
(62) Shim, J. W.; Gu, L. Q. *Anal. Chem.* **2007**, *79*, 2207−2213.
(63) Rambhav, S.; Ramachandran, L. K. *Indian J. Biochem. Biophys.* **1972**, *9*, 225−229.

crude product based on 2-aminoethyl gramicidate. ESI-MS in negative mode showed a major peak at $m/z = 1881.68$ corresponding to $[M - H]^-$ of the product.

Synthesis of Desethanolamine Gramicidin. We dissolved 4 mg (2.1 μmol) of 2-hydroxyethyl gramicidate in 292 μL MeOH. Separately, 15.4 mg (47.5 μmol) of Cs_2CO_3 was dissolved in 126 μL of H_2O, and this aqueous solution was added to the solution of 2-hydroxyethyl gramicidate. The reaction was stirred for 3 days at 23 °C. After acidifying the reaction mixture to pH 2 by dropwise addition of 1 M HCl, the solution was concentrated. The resulting precipitate was isolated to yield 97% of crude product based on 2-hydroxyethyl gramicidate. ESI-MS in positive mode revealed a major peak at $m/z = 1836.61$ corresponding to the expected $[M + H]^+$ of the product.

Synthesis of Taurinyl Gramicidate (2). We dissolved 4 mg (2.2 μmol) of desethanolamine gramicidin in 0.3 mL of anhydrous THF. We added 34.1 μL (237.6 μmol) of Et_3N and flushed the flask with N_2. The reaction vessel was cooled to 0 °C, and 1.2 μL of ethyl chloroformate was added. The solution was stirred at 0 °C for 3.5 h, and then a solution of 1.7 mg of taurine (dissolved in 30.0 μL of H_2O) was added to the solution containing desethanolamine gramicidin. The reaction was stirred for 30 min at 0 °C, warmed to 23 °C, and stirred an additional 12 h. The solution was concentrated *in vacuo* and purified by silica chromatography (9:1 DCM/MeOH) to give an overall isolated yield (over four steps) of 41% relative to gA. ESI-MS revealed a major peak at $m/z = 1944.79$ corresponding to the expected $[M + H]^+$ of the product.

Synthesis of Gramicidamine (3). Desethanolamine gramicidin A (5 mg, 2.7 μmol) and triethylamine (4.4 μL, 30 μmol) were added to 0.2 mL of dry DCM, and the resulting mixture was stirred and cooled to 0 °C. After ethyl chloroformate (1 μL, 10.8 μmol) was added to the cooled mixture, the reaction was stirred for 3.5 h at 0 °C. Mono-*tert*-butyloxycarbonyl-protected (BOC-protected) ethylenediamine was dissolved in 0.1 mL of dry DCM, cooled to 0 °C, and added to the desethanolamine gramicidin mixture. The resulting mixture was stirred for 30 min at 0 °C and then at room temperature for 8 h. After concentration to dryness, the BOC-protected gramicidamine was purified using preparative silica chromatography (9:1 DCM:MeOH as eluent). ESI-MS in negative mode showed a major peak at $m/z = 1979.66$ corresponding to the expected $[M - H]^-$ of the product.

A mixture of 1 mL of 1:1 DCM:trifluroacetic acid (TFA), 0.1 mL of dimethyl sulfide, and 0.02 mL of ethanedithiol was cooled to 0 °C. BOC-protected gramicidamine (2 mg, 1 μmol) was added to this DCM:TFA mixture. The reaction was allowed to warm up to room temperature and stirred for 3 h. The solvent was evaporated, and the crude mixture was dissolved in 2 mL of 2:1 DCM:MeOH. The mixture was added dropwise to 100 mL of water while stirring at 25 °C. The resulting precipitate was collected by filtration. ESI-MS showed a major peak at $m/z = 1881.62$ corresponding to the expected $[M + H]^+$ of the product. The overall yield of **3** was 74% from desethanolamine gramicidin A.

Molecular Modeling. The molecular mechanics calculations shown in Figure 2 were performed using MacroModel (version 7.5, Schroedinger, Inc.) with energy minimizations (using MM2 force field parameters) in water.[64] We constructed **1** and **2** *in silico* by modification of the C-termini of the crystal structure of gA (1GRM) in MacroModel. The first 14 residues of the peptide were fixed during the conformational analyses since they represent residues most likely embedded in the bilayer. After performing 5000 iterations of conformational analyses each for **1** and **2**, we examined the structures of the 20 lowest energy conformations calculated for **1** and **2** and found they were all very similar to the structures shown in Figure 2. We estimated the distance from the pore of the negative charge in **1** and **2** by measuring the distance of the sulfur atoms to a fixed point in space near the opening of the pore (located at half the distance between the α-proton of Leu14 and the α-proton of Trp11). To determine the maximum distance that the charge can exist from the pore in **1** and **2**, we created a hypothetical structure *in silico* for **1** and **2** with spacers (Figure 2A) in their fully extended conformation and measured the distance between the sulfur atoms and this same fixed point in space near the opening of the pore.

Formation of Planar Lipid Bilayers. We formed most planar lipid bilayers with the "folding technique." We used a Teflon film (Eastern Scientific Inc, pore diameter 0.1−0.2 mm) pretreated on each side with 2.5 μL of 5% hexadecane in pentane and air-dried. This film was mounted using vacuum grease (Dow Corning, High vacuum grease) to a custom-made Teflon chamber separating two buffer compartments each with a volume capacity of 4 mL.[44] After addition of 1 mL of electrolyte (0.01 to 1.00 M KCl buffered with HEPES pH 7.4) to each compartment, lipids were spread from a solution in pentane onto the surface of the electrolyte solutions (specifically, we added 4−6 μL from 25 mg mL^{-1} solution DiPhyPC or from 6.25 mg mL^{-1} each of 50% DOPS and 50% POPE or from 25 mg mL^{-1} DODAP mixed with 25 mg mL^{-1} DiPhyPC in a 1:9 ratio on top of the recording buffer in the bilayer chamber). Three additional milliliters of electrolyte solution were added to each side of the chamber to raise the liquid levels above the aperture. We formed the bilayers from apposition of two monolayers of lipids using the method described by Montal and Mueller[65] Briefly, bilayers were obtained by consecutively raising the liquid level in each compartment until the pore was completely covered by electrolyte. If at this point the pore was not closed by a lipid bilayer, and then the liquid level in one or both compartments was lowered below the pore level by aspirating electrolyte into a 3 mL syringe, followed by raising the electrolyte solution again. This cycle was repeated until a bilayer was obtained that had a minimum capacitance of 70 pF and until the resulting membrane was stable (i.e., no significant current fluctuations above the baseline noise level) in the range of ±200 mV applied potential for several minutes.

Planar lipid bilayers were also made with the "painting technique". We pretreated each side of a pore in a bilayer cup (Warner Instruments, Delrin perfusion cup, volume 1 mL, pore diameter 250 μm) with ~2 μL of a 25 mg mL^{-1} solution of DiPhyPC in hexane. After adding recording buffer (0.01 M KCl to 1.00 M KCl buffered with HEPES, pH 7.4) to both compartments of the bilayer setup, we "painted" a solution of 20 mg mL^{-1} DiPhyPC in n-decane over the pore by using a paint brush with a fine tip. We followed the thinning of the decane droplet to form a planar bilayer by monitoring the capacitance of the bilayer. In case the decane droplet did not thin out spontaneously, we bubbled air into the chamber underneath the pore. The rise of these air bubbles in the vicinity of the pore usually helped to thin out the decane/lipid droplet.[44] After verifying that bilayers were stable for several minutes (in the range of ±200 mV applied voltage) and that the capacitances were above 80−90 pF, we added gA (4−8 μL from 1 ng mL^{-1} in ethanol), derivatives **1** or **2** (2−10 μL from 100 ng mL^{-1} in ethanol), or derivative **3** (4−10 μL from 100 ng mL^{-1} in ethanol) directly to the bilayer chambers.

Ion Channel Measurements. We performed single channel recordings in "voltage clamp mode" using Ag/AgCl electrodes (Warner Instruments) in each compartment of the bilayer chambers. Data acquisition and storage was carried out using custom software in combination with either an EPC-7 patch clamp amplifier from List Medical Electronic (set at a gain of 10 mV pA^{-1} and a filter cutoff frequency of 3 kHz) or a Geneclamp 500 amplifier from Axon Instruments (with a CV-5B 100GU headstage, set at a gain of 100 mV

(64) It is well known that charged derivatives of gA do not cross lipid bilayers. This characteristic is attributed to the energetic cost of exposing a charge to the hydrophobic core of a bilayer. Therefore, the negative charge of the sulfonate group will likely favor an aqueous environment energetically over the hydrophobic bilayer environment. It is also known that gramicidin pores cause thinning of bilayers, and therefore the C-terminus of gA should be accessible to an aqueous environment. On the basis of these considerations, we calculated the energy minimized structures in water.

(65) Montal, M.; Mueller, P. *Proc. Natl. Acad. Sci. U.S.A.* **1972**, *69*, 3561−3566.

(66) More precisely, these mean current values were obtained from at least two indpendent experiments by fitting a Gaussian function to histograms of the current from the original current versus time traces.

pA^{-1} and filter cutoff frequency of 1 kHz). We used the EPC-7 amplifier for most folded bilayers and the Geneclamp 500 amplifier for most painted bilayers. The data acquisition boards for both amplifiers were set to a sampling frequency of 15 kHz. All current traces shown in the figures were further filtered using a digital Gaussian low-pass filter with a cutoff frequency of 30 Hz. The current traces we used to generate all data that was recorded at applied potentials $\leq$50 mV were filtered at 10 Hz.

We performed the analysis of the single channel current traces by computing histograms of the currents from the original current−time traces with ClampFit 9.2 software from Axon Instruments. From these histograms we extracted the main current values by fitting a Gaussian function to the peaks in the histograms. All gramicidin molecules showed a predominant conductance and occasionally subconductance states (i.e., single channel currents that were smaller than the main current values). Single channel conductances reported in this paper always refer to the main conductance state (i.e., to the dominant peaks in the current histograms).

Acknowledgment. This work was supported by a National Science Foundation CAREER Award (M.M., grant No. 449088) and by a research grant from IMRA America and AISIN USA as well as seed funds from the College of Engineering, University of Michigan. This work was also supported by the UCSD Academic Senate, a Hellman Faculty Fellowship for J.Y., and the UCSD Center for AIDS Research (NIAID 5 P30 AI36214).

JA0711819